DOI: 10.1002/cbic.200700553

The Inner-Shell Film: An Immediate Structure Participating in Pearl Oyster Shell Formation

Zhenguang Yan,[a] Zhuojun Ma,[a] Guilan Zheng,[a] Qiaoli Feng,[a] Hongzhong Wang,[a] Liping Xie,*[a, b] and Rongqing Zhang*[a, b]

In mollusks, the inner shell film is located in the shell-mantle zone and it is important in shell formation. In this study, we found that the film was composed of two individual films under certain states and some columnar structures were observed between the two individual films. The inner shell film was separated with the process of ethylenediaminetetraacetic acid (EDTA) treatment and the film proteins were extracted. Amino acid analysis showed that the film proteins may consist of shell framework proteins. The calcite crystallization experiment showed that the film proteins could inhibit the growth of calcite, while the $CaCO_3$ precipitation experiment showed that the film proteins could accelerate the rate of $CaCO_3$ precipitation. All these results suggested that the film plays an important role in shell formation. It may facilitate the aragonite formation by inhibiting the growth of calcite and accelerate the shell growth by promoting the precipitation of $CaCO_3$ crystals.

Introduction

The molluscan shell is composed of an outer uncalcified periostracum and inner calcified layers. The extrapallial fluid (EF) fills in the space between the calcified layer and the mantle. Some macromolecules that are involved in shell formation are secreted by the outer mantle epithelium. In terms of mantle–shell interactions, the zone between the mantle and the shell is obviously of great importance. A thin organic film named the innermost shell lamella (ISL) in some studies[1,2] tightly adheres to the inner surface of the shell.[3,4] This has been observed in Arcoid bivalves outside the pallial line[5] and in *Mercenaria mercenaria* and *Rangia cuneata* within the pallial line.[1,6] Generally, the film adheres to the calcified layer of the shell so firmly that it cannot be removed unless treated with ethylenediaminetetraacetic acid (EDTA). A previous study showed that the film may play an intermediary role in shell formation or dissolution.[1] In the pearl oyster *Pinctada fucata*, an organic sheet was observed in pearl sac-nacre preparation.[7] However, no further characterization was been performed.

Among the previous studies on the mechanism of shell formation, many works focused on the calcified layers of the shell, that is, the outer prismatic layer and the inner nacreous layer (nacre). The former consists of the calcitic polymorph of $CaCO_3$, whereas the latter is formed from aragonite tablets or lamella. The nacre is identical to the pearl in nature and it has attracted much attention in material science because of its unusual properties.[8–10] Among the factors involved in molluscan biomineralization, a small quantity of proteins occluded in the calcified layers is thought to play a critical role in shell formation. Heretofore, several nacreous proteins have been isolated from the pearl oyster nacre, and their functions involved in biomineralization have been investigated.[11–15] One of their distinct functions is that the nacreous proteins can inhibit the growth of calcite, and perhaps in such a way may facilitate the growth of the less thermodynamically stable aragonite phase.[16]

In the present study, we found that a thin organic film indeed forms the inner surface of the shell in *Pinctada fucata*. Furthermore, in a few cases, a two-layer structure of the film was definitely observed in the extrapallial zone of the shell. The analysis of the amino acid composition indicated that the film proteins may consist of shell framework proteins. The in vitro $CaCO_3$ crystallization and precipitation experiments showed that the film proteins not only could inhibit the growth of calcite, but also could promote the precipitation of $CaCO_3$.

Results

SEM observation of the film

To detect the film in the pearl oyster, the shell section samples were observed with SEM. Comparison of the samples processed with and without EDTA revealed a film that forms the inner surface of the shell (Figure 1). As shown in Figure 1, the film exhibits a different appearance in different zones of the shell. In most cases, the film of the central and extrapallial zone has a similar appearance, where a distinct polygonal

[a] *Z. Yan, Z. Ma, G. Zheng, Q. Feng, Prof. H. Wang, Prof. L. Xie, Prof. R. Zhang*
Institute of Marine Biotechnology
Department of Biological Sciences and Biotechnology, Tsinghua University
Beijing 100084 (China)
Fax: (+86) 10-62772899
E-mail: lpxie@mail.tsinghua.edu.cn
rqzhang@mail.tsinghua.edu.cn

[b] *Prof. L. Xie, Prof. R. Zhang*
Protein Science Laboratory of the Ministry of Education, Tsinghua University
Beijing 100084 (China)

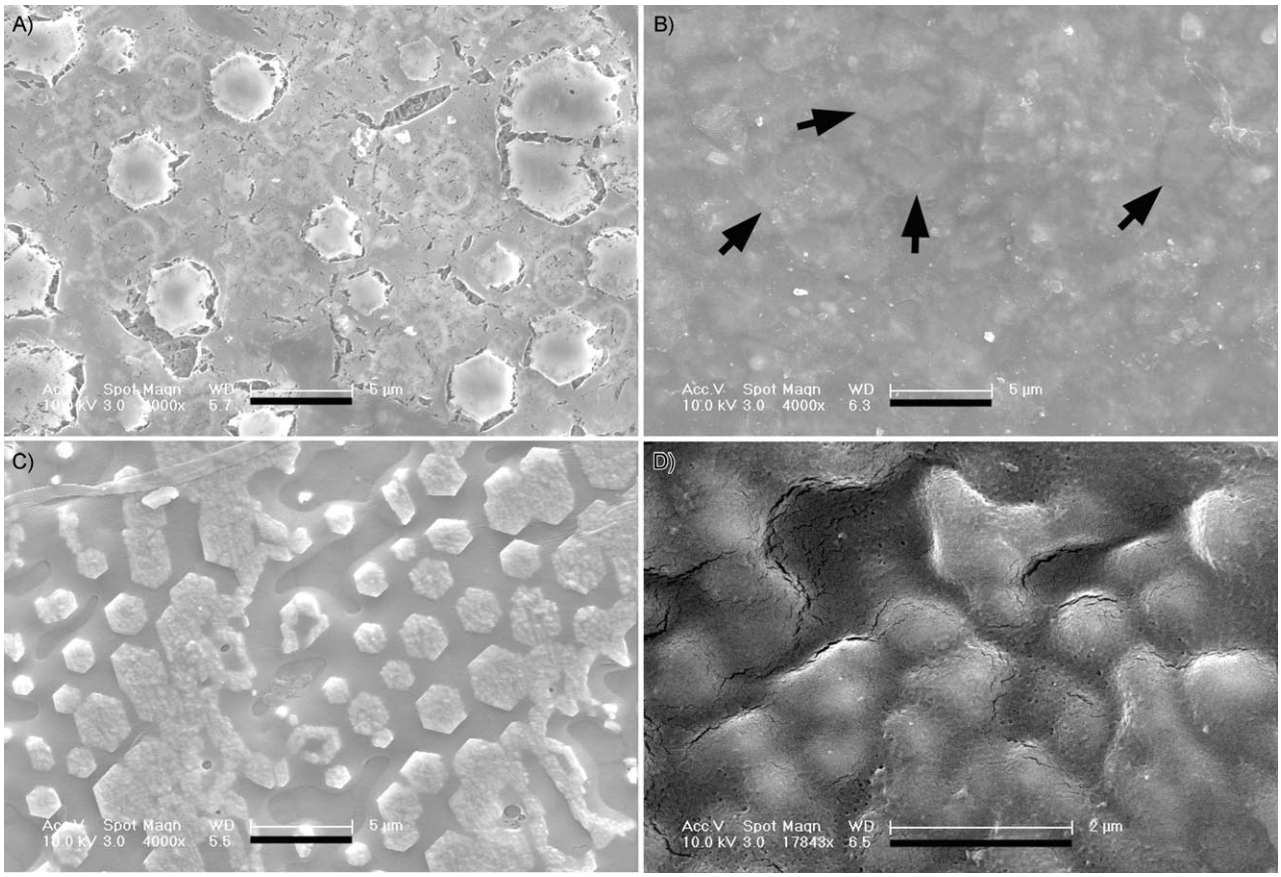

Figure 1. SEM images of inner shell film (in situ). The samples were treated without the use of EDTA. A and B) The appearance of the film of the central zone. Some distinct and vague shapes (indicated by arrows) of aragonite are shown. C and D) The appearance of the film of the extrapallial zone. Some distinct shapes of aragonite are shown in C, whereas some underlying round-like shapes are shown in D. The bars are 5 µm in A, B, and C, and 2 µm in D.

shape can be seen (Figure 1 A and C). This suggested that the underlying substance is aragonite crystal. However, in a few cases, the film in these two zones seems too thick to easily distinguish the shape of the underlying substance (Figure 1 B and D). In these cases, a vague polygonal shape of the underlying aragonite tablets can be seen in the central zone (Figure 1 B, indicated by arrows), whereas a vague round-like shape can be observed in the extrapallial zone (Figure 1 D). When the film was reversed with forceps, some distinct aragonitic tablets were observed. From the sample of the partially-reversed film (Figure 2), we can see that the aragonitic tablets not only form the surface of the nacre (Figure 2, left) but also adhere to the shell-facing surface of the film (Figure 2, right).

To observe the inside structure of the film, some split samples were tentatively prepared. The results showed that some structures could be observed through the split gap. In most cases, aragonite could be seen directly from the gap (data not shown), whereas in a few cases, another film was found from the gap (Figure 3 A). The aragonite could be observed from the gap of the underlying film (Figure 3 B). In some samples, the mantle-facing film curled back and some columnar structures sandwiched between the two films were revealed (Figure 4). When the samples were treated with 0.5 M EDTA for one hour, the columnar structures were dissolved (Figure 4 C and D). In addition, the chemical composition analysis by EDS showed that the columnar structures were composed of carbon, oxygen, and calcium (Figure 4 E).

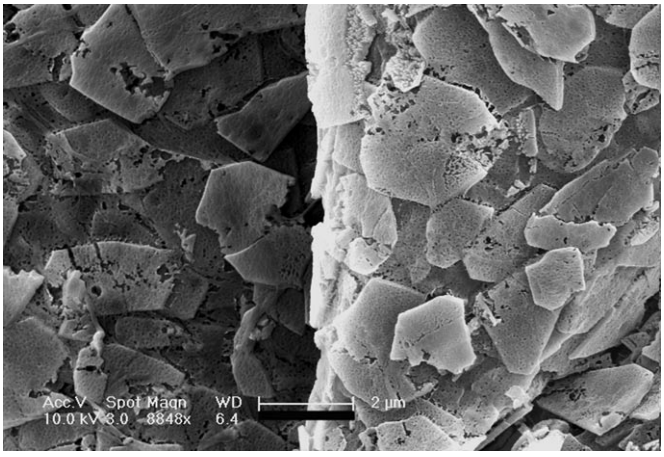

Figure 2. SEM images of the nacre (left) and the shell-facing surface of the film (right). The film was reversed with forceps. Bar, 2 µm.

Amino acid compositions of the film proteins

After being treated with EDTA, the film was separated from the shell (Figure 5), and the film proteins were extracted. The

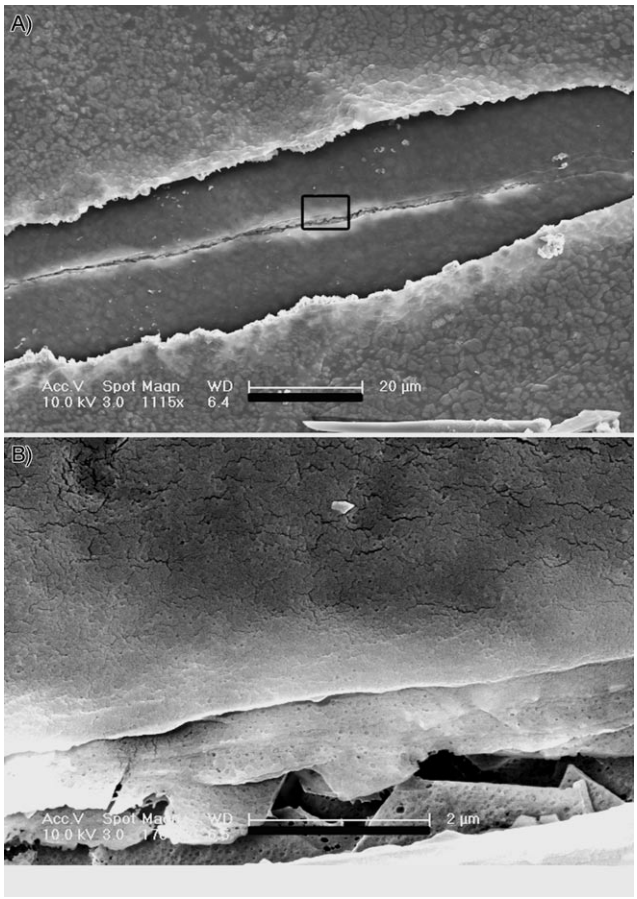

Figure 3. SEM images of the split films in the extrapallial zone. A) Split films. The upper film (mantle-facing film) has a bigger gap and the lower film (shell-facing film) has a slight gap. B) Enlargement of the box in A. Some aragonitic tablets with polygonal edge were observed through the gap. The bars in panels A and B are 20 µm and 2 µm.

amino acid analysis showed that both the soluble and insoluble proteins of the film are rich in Gly and Ala, and they are similarly composed of sixteen kinds of amino acids (Table 1).

Table 1. Amino acid analysis of the soluble and insoluble film proteins.

Amino acid	Soluble film proteins [mol%]	Insoluble film proteins [mol%]
Asp	10.45	9.40
Glu	3.00	2.52
Gly	37.67	43.76
Ala	18.25	16.12
Thr	0.98	0.89
Ser	6.23	5.89
Val	2.28	1.93
Met	1.19	0.95
Ile	1.06	1.02
Leu	6.57	6.35
Tyr	1.97	1.78
Phe	2.34	1.92
Lys	2.12	1.83
Arg	4.12	3.90
His	0.19	0.19
Pro	1.58	1.55

The total percentage of Gly and Ala in soluble and insoluble proteins of the film is 55.92 mol% and 59.88 mol%, respectively. No Cys was found in the film proteins.

Inhibition activity of the soluble proteins of the film on calcite growth

To investigate the effects of the soluble proteins of the film on the growth of calcite, the crystals formed in vitro were examined by SEM. In the presence of the soluble film proteins, the morphology of calcite was drastically changed in a concentration-dependent manner, whereas the crystals obtained in control experiments were the typical rhombohedra of calcite (Figure 6). The film proteins could etch the edge of calcite at low concentrations and round the calcite at higher concentration. In addition, the size of calcite crystals decreased apparently in the presence of the soluble film proteins.

Soluble film proteins' promotion of $CaCO_3$ precipitation

A series of precipitation experiments with or without the soluble film proteins were performed (Figure 7). The effect of the soluble film proteins on the rate of precipitation of $CaCO_3$ was determined by recording the increase of absorbance at 570 nm in a saturated $CaCO_3$ solution. The initial absorbance, which depended on the $CaCO_3$ concentration, was about 0.032, where $CaCO_3$ was precipitated at room temperature in less than 5 min. When the soluble film proteins were added to the saturated $CaCO_3$ solution, the absorbance of solution at 570 nm significantly increased in a concentration-dependent manner compared with that of the control (shown in Figure 7). Water or BSA could not affect the absorbance (data not shown).

Discussion

The molluscan biomineralization system is composed of the shell, EF, and mantle.[19] The organic film that is sandwiched between the shell and the EF is located on the inner surface of the shell.[1] Based on the location, the film is presumably important in shell formation. However, this film has not been obviously sufficiently researched.

In the present study, we investigated the morphology and structure of the organic film. The results showed that the film covers the inner surface of the pearl oyster shell. The film is not homogeneous in different zones of the shell. Even in the same zone, the film may have a different appearance. This suggested that the film is a dynamic structure, which agrees with the previous studies in which the film was shown to vary considerably in thickness.[1,2] When the film was removed with the use of EDTA, the typical polygonal aragonitic tablets were observed (Figure 2). Thus, we can conclude that the film indeed exists in the pearl oyster. From the partially-reversed film sample, we can see that some aragonitic tablets were firmly adhered to the film and they were reversed together with the film (Figure 2, right). This is consistent with a previous study[1] in which the film was firmly adhered to the calcified layer.

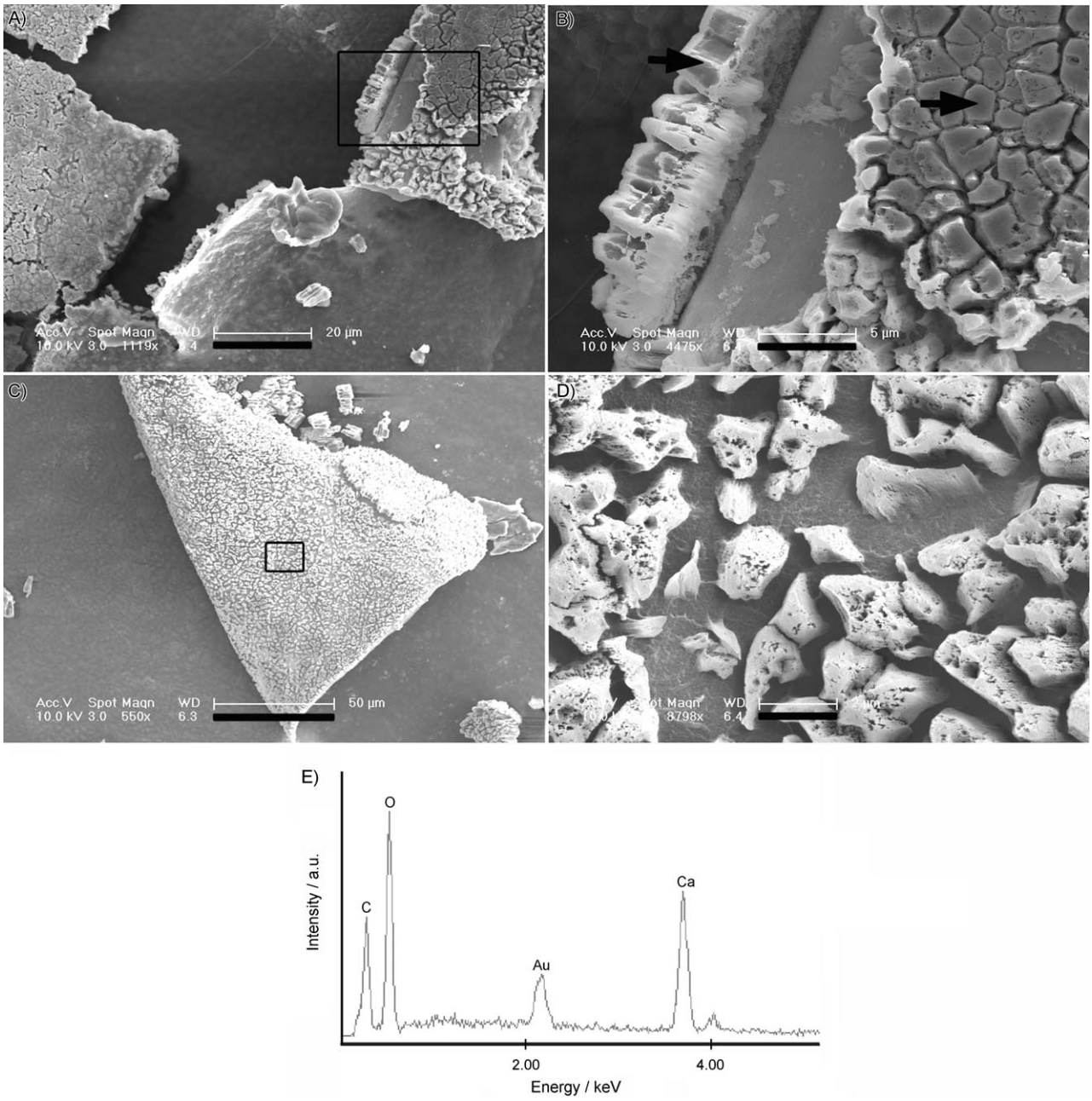

Figure 4. SEM images of the columnar structures sandwiched between the two films. A and C) Shell sections treated with EDTA for 30 min and 60 min, respectively, and the mantle-facing film curled back. B) Enlargement of the box in A to show the columnar structures (indicated by arrows). D) Enlargement of the box in C to indicate that the columnar structures were dissolved. E) EDS analysis of the columnar structures in B. The bars are 20 µm in A, 5 µm in B, 50 µm in C and 2 µm in D.

We noted that, in the extrapallial zone, the underlying substance of the film in a few cases (Figure 1D) is round-like in shape and it is unlike those of the other samples (Figure 1C). Therefore, we prepared the split samples of this zone to reveal the possible difference of the underlying substance. Some slight or bigger gaps were made on the surface of the film. Generally, distinct aragonites could be seen through the split gap of the film (data not shown). In a few cases, however, when the film was split, another underlying film was observed (Figure 3). It seems that, in these samples, the so-called film actually consists of two films, including a shell-facing film and a mantle-facing film. As this special structure is not present in all cases, it may be a dynamic structure that occurs under certain states. In some samples, where the mantle-facing film has cracked and curled back from the surface of the shell, the inner surface of the mantle-facing film can be examined in detail (Figure 4). Some columnar structures were observed sandwiched between the two films. This also explains why the underlying substance of the extrapallial zone in a few cases is not polygonal (the shape of aragonite), but round-like in shape (Figure 1D). As the columnar structures could be dissolved with EDTA treatment, and in view of the mineralogy of the

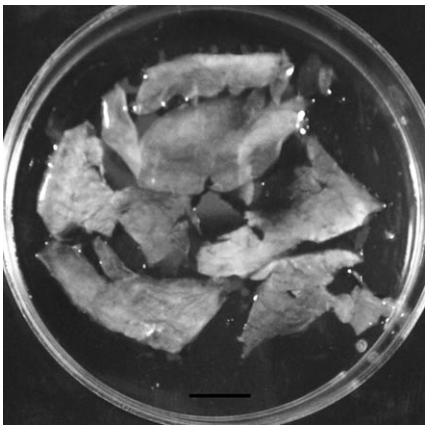

Figure 5. Macrophotography images of the film detached from the shell. Bar, 5 mm.

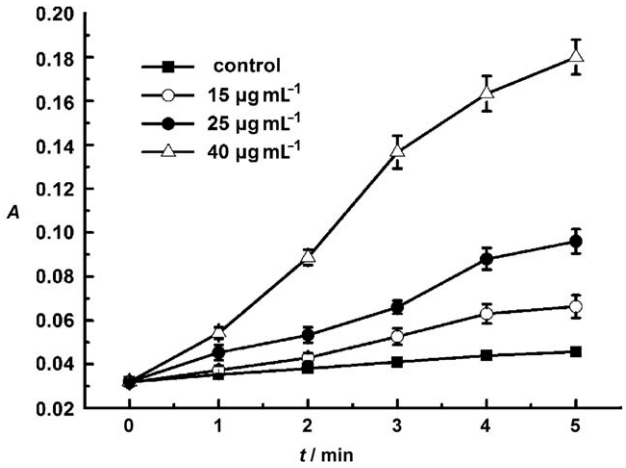

Figure 7. Promotion activity of the film proteins on $CaCO_3$ precipitation. Changes in the turbidity of the assayed solutions are shown. The vertical axis: absorbance at 570 nm.

shell and the results of EDS analysis, we inferred that the columnar structures might be composed of calcium carbonate. Further characterization is ongoing.

As for the amino acid analysis of the film, previous work[1] has determined the quantity of the total amino acid in the film. However, no study on the determination of the global amino acid composition has been reported. In this present study, we performed the global amino acid analysis of the soluble and insoluble film proteins and found that the two fractions are actually identical in nature because of the similar

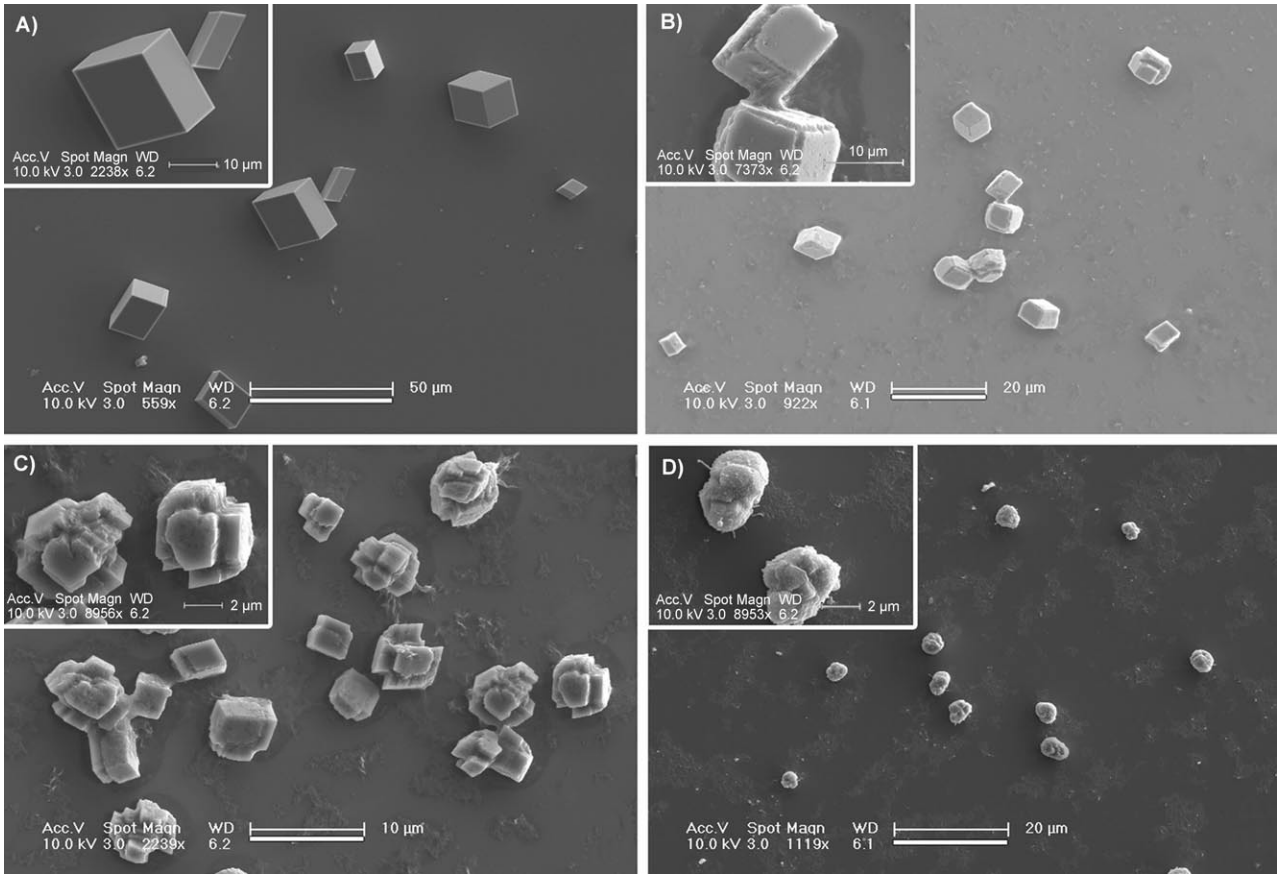

Figure 6. SEM images of morphological modification in calcite crystals induced by the film proteins. A) Typical rhombohedra of calcite formation in the presence of filtrate (control). B, C and D are images showing the morphological modification of calcite crystals in the presence of the film proteins at the concentrations of 15, 25 and 40 μg mL^{-1}, respectively. The insets in each image are enlargements of portions of A, B, C, and D. The bars are 50 μm in A, 20 μm in B and D, and 10 μm in C.

amino acid composition. Among the biomacromolecules related to shell biomineralization, the shell matrix proteins have been extensively studied.[16,20,21] Two classes of proteins (soluble acidic proteins[22–25] and insoluble framework proteins[18,26]) have been identified according to their solubility in aqueous solution after demineralization.[19] They are considered to play an important role in regulation of crystal growth.[27] The soluble proteins are characterized by the predominance of acidic glycoproteins, whereas the insoluble framework proteins which are thought to provide a framework where the mineralization occurs,[28] are rich in Gly and Ala residue content. Therefore, based on the results of the amino acid analysis and the location of the film, we inferred that the film proteins may consist of the shell insoluble framework proteins or their precursors, and during shell formation, the film proteins are integrated into the shell in a certain manner. In addition, it is a little surprising that no Cys residue was detected in the film proteins. As some Cys residues have been found in shell proteins,[20] especially in the framework proteins of *Pinctada fucata*,[29] we inferred that there must be some other framework proteins that differ from the film proteins in the shell.

After partial biochemical characterization, we investigated the functions of the film proteins in mineralization. The in vitro crystallization experiment showed that the growth of calcite can be inhibited by the film proteins, whereas the precipitation experiment showed that the film proteins have drastic effects on promoting the rate of $CaCO_3$ precipitation. In addition, the Raman spectra of the crystal precipitation shown in Figure 6C and D showed that the crystals are all calcite (data not shown). This suggested that the film proteins can only affect the morphology of calcite. The functions of the shell framework proteins (silk-like proteins[28]) in biomineralization have been described in previous studies.[8] Besides participating in the construction of the shell's organic framework, they are considered as an inhibitor of mineralization to prevent uncontrolled crystallization during shell formation. The inhibition of calcite crystal growth by the film proteins in this study is consistent with previous work,[8] whereas the promotion activity of these proteins was demonstrated for the first time. In conclusion, we deduced that, by attaching to the inner surface of nacre, the organic film may be multifunctional in regulating shell formation. In detail, the film proteins may facilitate the formation of aragonitic nacre by inhibiting the growth of calcite and may accelerate shell growth by promoting the precipitation of $CaCO_3$ crystals.

Experimental Section

Materials and equipment: The water used in all experiments was ultrapure water filtered through a Milli-Q column supplied by Millipore (USA). Fresh shells of pearl oysters were obtained from Guofa Pearl Farm (Beihai, Guangxi Province, China). Glutaraldehyde, glycerol, ammonium sulfate, $CaCO_3$, $NaHCO_3$, and $CaCl_2$ as well as reagents for SDS-PAGE and amino acid analysis were purchased from Sigma. A BCA assay kit was purchased from Pierce (USA). EDTA, fluid nitrogen, and slides were purchased from the Beijing Reagent Corp. (China). A centrifugal filter unit was purchased from Millipore (USA). The centrifuge tube was purchased from Nalgene (USA) and the syringe filter (0.2 μm) was purchased from Whatman (England). Dialysis tubes (MWCO = 3500) were purchased from Membrane Filtration Products Inc. (USA). Samples were freeze-dried by using a Christ ALPH A1–2 freeze dryer (Germany). Centrifugation was performed with a Hitachi CR21G II centrifuge (Japan). Gels were run on a Mini-protean 3 apparatus from BioRad Laboratories. The amino acid composition was analyzed on a Beckman System 6300 automated amino acid analyzer, which was equipped with a 25-cm column and quantified by ninhydrin reaction. $CaCO_3$ precipitation experiments were performed with a SPECORD 200 spectrophotometer (Analytik Jena, Germany). The scanning electron microscope (SEM) images were obtained by using a SIRION 200 SEM (PEI) equipped with an energy dispersive X-ray spectroscopy (EDS) system.

Samples preparation for SEM observation: After being cleaned, the shells were cut to proper sections in terms of different zones. Each section was rinsed with EDTA (0.5 M) and washed with water. Then, the films of some sections were reversed with forceps to observe the surface of the nacre and the nacre-facing surface of the film. Alternatively, the film was tentatively split with a needle to observe the inside structure. The control samples were only washed with water. After these treatments, all the sections were immersed in glutaraldehyde (2.5%) for 1 h. Then, the sections were washed with water and immersed in glycerol solution (30%) for 3 h. After that, the sections were frozen in fluid nitrogen and subsequently freeze dried. The samples were coated with gold before imaging. Some samples were characterized by EDS.

Isolation of the film proteins: The shells were cleaned as described above. After being rinsed with EDTA (0.5 M) for 30 min, the film was separated from the shell. The detached film was rinsed again with EDTA (0.5 M) until it was decalcified completely. The decalcified film was washed extensively with water and collected by centrifugation. After that, the film was ground in a mortar with continuous addition of fluid nitrogen. The powder-like products were dissolved in water and the soluble and insoluble fractions were collected by centrifugation. The insoluble fraction was stored at −20 °C, while the soluble fraction was subjected to ammonium sulfate fractionation. The precipitate (by 90% saturation) was dissolved in water, and then it was extensively dialyzed against water and concentrated by ultrafiltration (Millipore; cut-off, 5 kDa). The soluble proteins of the film were detected with reduced and unreduced SDS-PAGE.

The protein yields were measured using a bicinchoninic acid (BCA) assay kit (Pierce) with bovine serum albumin (BSA) standard. Briefly, each standard or sample (10 μL) was added into microwell plate wells. The working reagent (200 μL) was added to the wells and mixed on a shaker. After incubation at 37 °C for 30 min, the plate was cooled to room temperature and the absorbance was measured. The protein concentration of each sample was determined using the standard curve.

Amino acid analysis of the film proteins: In preparation for amino acid analysis, the soluble and insoluble fractions of the film were hydrolyzed under vacuum in HCL (6 N) at 110 °C for 24 h. Then, samples and amino acid standards were analyzed on the amino acid analyzer. The amino acid compositions of the samples, expressed as mole percentage, represent the average of three independent determinations, respectively.

Inhibition of calcite growth: The calcitic crystallization solution was prepared according to a previous study[17] by purging a stirred aqueous suspension of $CaCO_3$ with CO_2 for 4 h. Then, excess solid $CaCO_3$ was removed by filtering (0.2 μm) and subsequently, the fil-

trate was purged with CO_2 for another hour. Crystallization experiments were carried out by adding samples to the freshly prepared crystallization solution on a slide at 20 °C. After 24 h, the crystallization solution was removed and the crystals were characterized.

Promotion of $CaCO_3$ precipitation: According to the method described previously,[18] the effect of the soluble film proteins on $CaCO_3$ precipitation from its supersaturated solution was examined. In brief, sample solution (10 μL) was mixed with $NaHCO_3$ (100 μL, 40 mM, pH 8.7). After the addition of $CaCl_2$ (100 μL, 20 mM) to the mixed solution, the formation of $CaCO_3$ precipitates was monitored by recording the turbidity. Changes in the turbidity of the solutions were measured every minute for 5 min by the absorbance at 570 nm using a spectrophotometer.

Acknowledgements

This work was financially supported by Grants 30530600, J0630647 and the National High Technology Research and Development Program of China (2006AA09Z441 and 2006AA09Z413).

Keywords: biomineralization · *Pinctada fucata* · proteins · shell film · structural biology

[1] M. E. Marsh, R. L. Sass, *J. Exp. Zool.* **1983**, *226*, 193–203.
[2] M. E. Marsh, *J. Exp. Zool.* **1986**, *239*, 207–220.
[3] M. Rousseau, E. Lopez, A. Coute, G. Mascarel, D. C. Smith, R. Naslain, X. Bourrat, *J. Struct. Biol.* **2005**, *149*, 149–157.
[4] H. A. Lowenstam, S. Weiner, *On Biomineralization*, Oxford University Press, New York, **1989**.
[5] T. R. Waller, *Smithson. Contrib. Biol.* **1980**, *313*, 1–58.
[6] J. M. Neff, *Tissue Cell* **1972**, *4*, 591–600.
[7] K. Wada, *Biomineralisation* **1972**, *6*, 141–159.
[8] L. Addadi, D. Joester, F. Nudelman, S. Weiner, *Chem. Eur J.* **2006**, *12*, 980–987.
[9] F. Marin, G. Luquet, *C. R. Palevol* **2004**, *3*, 469–492.
[10] F. Nudelman, B. A. Gotliv, L. Addadi, S. Weiner, *J. Struct. Biol.* **2006**, *153*, 176–187.
[11] H. Miyamoto, T. Miyashita, M. Okushima, S. Nakano, T. Morita, A. Matsushiro, *Proc. Natl. Acad. Sci. USA* **1996**, *93*, 9657–9660.
[12] T. Samata, N. Hayashi, M. Kono, K. Hasegawa, C. Horita, S. Akera, *FEBS Lett.* **1999**, *462*, 225–229.
[13] C. Zhang, S. Li, Z. Ma, L. Xie, R. Zhang, *Mar. Biotechnol.* **2006**, *8*, 624–633.
[14] M. Kono, N. Hayashi, T. Samata, *Biochem. Biophys. Res. Commun.* **2000**, *269*, 213–218.
[15] Z. Yan, G. Jing, N. Gong, C. Li, Y. Zhou, L. Xie, R. Zhang, *Biomacromolecules* **2007**, *8*, 3597–3601.
[16] M. Michenfelder, G. Fu, C. Lawrence, J. C. Weaver, B. A. Wustman, L. Taranto, J. S. Evans, D. E. Morse, *Biopolymers* **2003**, *70*, 522–533.
[17] G. Xu, N. Yao, I. A. Aksay, J. T. Groves, *J. Am. Chem. Soc.* **1998**, *120*, 11977–11985.
[18] M. Suzuki, E. Murayama, H. Inoue, N. Ozaki, H. Tohse, T. Kogure, H. Nagasawa, *Biochem. J.* **2004**, *382*, 205–213.
[19] S. Mann, *Biomineralization. Principles and Concepts in Bioinorganic Materials Chemistry*, Oxford University Press, New York, **2001**.
[20] L. Treccani, K. Mann, F. Heinemann, M. Fritz, *Biophys. J.* **2006**, *91*, 2601–2608.
[21] Z. Yan, Z. Fang, Z. Ma, J. Deng, S. Li, L. Xie, R. Zhang, *Biochim. Biophys. Acta Gen. Subj.* **2007**, *1770*, 1338–1344.
[22] G. Fu, S. Valiyaveettil, B. Wopenka, D. E. Morse, *Biomacromolecules* **2005**, *6*, 1289–1298.
[23] B. A. Gotliv, N. Kessler, J. L. Sumerel, D. E. Morse, N. Tuross, L. Addadi, S. Weiner, *ChemBioChem* **2005**, *6*, 304–314.
[24] I. M. Weiss, S. Kaufmann, K. Mann, M. Fritz, *Biochem. Biophys. Res. Commun.* **2000**, *267*, 17–21.
[25] F. Marin, R. Amons, N. Guichard, M. Stigter, A. Hecker, G. Luquet, P. Layrolle, G. Alcaraz, C. Riondet, P. Westbroek, *J. Biol. Chem.* **2005**, *280*, 33895–33908.
[26] C. Zhang, L. Xie, J. Huang, X. Liu, and R. Zhang, *Biochem. Biophys. Res. Commun.* **2006**, *344*, 735–740.
[27] S. Weiner, L. Addadi, *Trends Biochem. Sci.* **1991**, *16*, 252–256.
[28] L. Pereira-Mouries, M. J. Almeida, C. Ribeiro, J. Peduzzi, M. Barthelemy, C. Milet, E. Lopez, *Eur. J. Biochem.* **2002**, *269*, 4994–5003.
[29] S. Sudo, T. Fujikawa, T. Nagakura, T. Ohkubo, K. Sakaguchi, M. Tanaka, K. Nakashima, T. Takahashi, *Nature* **1997**, *387*, 563–564.

Received: September 17, 2007
Published online on March 28, 2008

